Perfect lensing with phase conjugating surfaces: Towards practical realization

Stanislav Maslovski[1] and Sergei Tretyakov[2]

[1]*Departmento de Engenharia Electrotécnica,*
Instituto de Telecomunicações - Universidade de Coimbra,
Pólo II, 3030 Coimbra, Portugal
[2]*Aalto University, School of Electrical Engineering,*
P.O. 13000, FI-00076 Aalto, Finland
E-mails: stas@co.it.pt, sergei.tretyakov@aalto.fi

(Dated: August 23, 2011)

It is theoretically known that a pair of phase conjugating surfaces can function as a perfect lens, focusing propagating waves and enhancing evanescent waves. However, the known experimental approaches based on thin sheets of nonlinear materials cannot fully realize the required phase conjugation boundary condition. In this paper we show that the ideal phase conjugating surface is in principle physically realizable and investigate the necessary properties of nonlinear and nonreciprocal particles which can be used to build a perfect lens system. The physical principle of the lens operation is discussed in detail and directions of possible experimental realizations are outlined.

I. INTRODUCTION

The *perfect lens*[1] is a device which focuses the field of a point source into a point, that is, the perfect lens focuses both propagating and evanescent fields. It is known[1] that a planar slab of the ideal Veselago medium[2] with the relative permittivity and permeability both equal to -1 has the perfect-lens properties because of the negative refraction phenomenon and the excitation of coupled surface plasmon-polaritons at the slab interfaces. Practical realization of such double-negative (DNG) materials is, however, a significant challenge, especially at optical frequencies, and, clearly, any realization will suffer from some imperfections. For example, metal-dielectric metamaterials have relatively high ohmic losses that are responsible for nonvanishing imaginary parts in the constitutive parameters of such volumetric artificial media.

There is, however, a possibility for a different realization of a perfect lens that does not require any volumetric metamaterials. Indeed, the physical effects necessary for perfect lensing happen at the lens interfaces, and not within the metamaterial volume. Therefore, if one realizes a *metasurface* at which the incident waves refract negatively, then a parallel pair of such planar sheets will mimic the operation of the Veselago lens for the *propagating* plane waves. Moreover, if this metasurface supports surface modes (surface plasmon-polaritons) within a wide range of the tangential propagation factors $k_t > k_0$ (where k_0 is the free space wavenumber), then also the impinging *evanescent* plane waves will interact resonantly with the sheets and will be tunneled through the lens with an enhanced amplitude, due to the electromagnetic coupling between the surface states excited on the sheets. Such subwavelength imaging with *linear* plasmon-polariton resonant grids was theoretically predicted and confirmed experimentally in a number of works.[3–7]

In 2003, we showed[8] that two parallel sheets with phase conjugating boundary conditions for tangential fields on the two sides of the sheets

$$\mathbf{E}_{t+} = \mathbf{E}_{t-}^*, \qquad \mathbf{H}_{t+} = \mathbf{H}_{t-}^* \tag{1}$$

have the necessary properties of the perfect lens outlined above. In these conditions that are written for the complex amplitudes of the time-harmonic fields (symbol * denotes complex conjugation operation) the indices $\pm$ indicate the field values on the two sides of an infinitely thin phase conjugating sheet.

Obviously, boundary conditions (1) cannot be realized using linear materials, and in the same paper[8] the use of three-wave mixing in a nonlinear layer was proposed as an approach to realization of this effect. Phase conjugation and "time-reversal" devices were studied also earlier for other applications. It is interesting that in the same year (2003) an experimental microwave realization of a phase conjugating layer was published[9] independently from our work.[8] Later, the concept of perfect lensing based on two nonlinear sheets was studied theoretically in Ref. 10. Alternative experimental realizations of nonlinear negative refraction effect were published in Refs. 11,12.

However, in known devices based on antenna arrays with mixers,[9] or sheets of nonlinear dielectrics,[10] or arrays of only electric or only magnetic particles with nonlinear insertions,[12] the phase conjugated ("time-reversed") products create waves propagating symmetrically to the both sides of the sheet, i.e., there appears a retrodirected wave

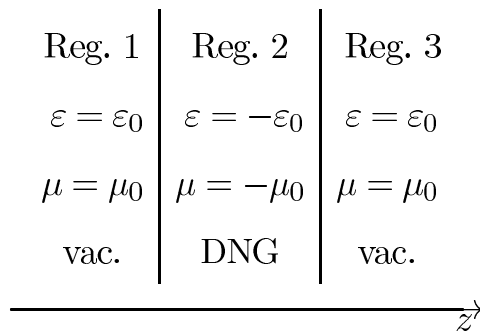| Reg. 1	Reg. 2	Reg. 3
$\varepsilon = \varepsilon_0$	$\varepsilon = -\varepsilon_0$	$\varepsilon = \varepsilon_0$
$\mu = \mu_0$	$\mu = -\mu_0$	$\mu = \mu_0$
vac.	DNG	vac.

$\overrightarrow{z}$

FIG. 1: An ideal Veselago lens: A planar slab of a double-negative (DNG) material with the medium parameters $\varepsilon = -\varepsilon_0$ and $\mu = -\mu_0$ in free space.

propagating back to the source. While the perfect lens operation can be theoretically approached even in such systems if the amplitudes of the nonlinear products tend to infinity in the assumption of nonphysical infinitely strong external pumping,[10] the ideal phase conjugating boundary conditions (6) cannot be realized within this scenario.

In this paper we discuss the physical meaning of the ideal complex-conjugation boundary conditions (1) and outline possible approaches for realization of such surfaces, which would potentially lead to creation of super-resolution lenses. The paper is organized as follows. In Section II we consider physical processes taking place at a phase conjugating boundary and demonstrate that such boundary may be equivalently represented with pairs of electric and magnetic surface currents reacting (nonlinearly) to the applied magnetic and electric fields. In Section III a realization of the phase conjugating boundary with an array of bi-anisotropic inclusions is proposed and studied and the necessary conditions on nonlinear susceptibilities of the inclusions are established. In Section IV a possible microwave design of such inclusions is proposed.

II. THE PHYSICAL MEANING OF THE COMPLEX-CONJUGATING BOUNDARY CONDITIONS

A. Complex-conjugating boundary and perfect lens

Let us start from outlining the idea from our paper in Ref. 8. Consider an ideal Veselago lens depicted in Figure 1. Let the relative permittivity and permeability of the medium surrounding the lens be equal to 1 and the relative parameters of the lens material to -1 at the working frequency ω, respectively. At the lens interfaces the tangential components of the fields satisfy the usual Maxwellian continuity conditions. One may notice that in this system the only difference between the time-harmonic [the time dependence is of the form $\exp(+j\omega t)$] field equations in the Veselago slab (region 2)

$$\nabla \times \mathbf{E} = j\omega\mu_0\mathbf{H}, \qquad \nabla \times \mathbf{H} = -j\omega\varepsilon_0\mathbf{E} \tag{2}$$

and the analogous equations in the free-space regions is the sign in front of the imaginary unit. A substitution

$$\mathbf{E}_{(\text{old})}, \mathbf{H}_{(\text{old})} \Rightarrow C\mathbf{E}^*_{(\text{new})}, C\mathbf{H}^*_{(\text{new})} \tag{3}$$

(C is an arbitrary constant; here and thereafter * denotes the complex conjugation) into the field equations in region 2 reformulates the problem in terms of the new field vectors in which the field equations become the same in all three regions:

$$\nabla \times \mathbf{E} = -j\omega\mu_0\mathbf{H}, \qquad \nabla \times \mathbf{H} = j\omega\varepsilon_0\mathbf{E}, \tag{4}$$

that are simply the Maxwell equations in free space. The boundary conditions on the two interfaces, however, are no more the standard continuity conditions, but they involve complex conjugation:

$$\mathbf{E}_{t_{(1,3)}} = C\mathbf{E}^*_{t_{(2)}}, \qquad \mathbf{H}_{t_{(1,3)}} = C\mathbf{H}^*_{t_{(2)}}. \tag{5}$$

The constant C describes the "transformation efficiency" of the nonlinear surface which transforms fields into the complex-conjugate state. In the known experimental realizations of phase conjugation in electrically thin layers (e.g., Ref. 12), the efficiency has been rather small. However, by choosing a small value of C in (5), we arrive at a structure

with asymmetric properties with respect to the two sides of the surface. Indeed, complex conjugating and dividing (5) by C^*, we see that in this case the weak fields inside the lens should be enhanced by the surface in the same rate as they are suppressed when the surface is excited from outside. For this reason we will concentrate on the simplest choice of $C = 1$, as in Ref. 8, described by the boundary conditions

$$\mathbf{E}_{t_{(1,3)}} = \mathbf{E}_{t_{(2)}}^*, \qquad \mathbf{H}_{t_{(1,3)}} = \mathbf{H}_{t_{(2)}}^*. \tag{6}$$

In this case the complex-conjugating surface has symmetric properties with respect to its two sides, and for the ideal lens operation the amplitudes of the field should not change across the sheets.

Now it becomes evident that the problem involving an ideal Veselago slab is mathematically equivalent to the problem dealing with a pair of conjugating surfaces in free space, provided that the field sources are outside of region 2. Therefore, in the latter system the field solutions are the same as in the Veselago slab, and because of this the physical phenomena taking place at the interfaces of region 2 are also the same: The propagating plane waves are refracted negatively at the interfaces, and the evanescent modes are enhanced due to the excitation of coupled surface plasmon-polariton pairs. In this regard, a pair of phase conjugating planes is indistinguishable from a perfect lens proposed by Pendry.[1] In what follows we concentrate on physical properties of such phase conjugating sheets.

B.   Plane-wave propagation across the phase conjugating sheet

Let us consider a single phase conjugating surface located at $z = 0$. We decompose the tangential electric and magnetic fields into plane waves at both sides of the surface:

$$\mathbf{E}_t(x, y)\Big|_{z=\pm 0} = \frac{1}{(2\pi)^2} \int\int \mathbf{E}_t(k_x, k_y)\Big|_{z=\pm 0} e^{-j(k_x x + k_y y)} \, dk_x dk_y, \tag{7}$$

$$\mathbf{H}_t(x, y)\Big|_{z=\pm 0} = \frac{1}{(2\pi)^2} \int\int \mathbf{H}_t(k_x, k_y)\Big|_{z=\pm 0} e^{-j(k_x x + k_y y)} \, dk_x dk_y. \tag{8}$$

It is easy to see that the boundary conditions (6) require that the plane-wave components satisfy

$$\mathbf{E}_t(k_x, k_y)\Big|_{z=+0} = \mathbf{E}_t^*(-k_x, -k_y)\Big|_{z=-0}, \tag{9}$$

$$\mathbf{H}_t(k_x, k_y)\Big|_{z=+0} = \mathbf{H}_t^*(-k_x, -k_y)\Big|_{z=-0}. \tag{10}$$

From these relations we immediately realize that the propagating modes refract negatively at the conjugating interface due to the change in the sign of *the tangential* component of the wave vector $\mathbf{k}_t = k_x \mathbf{x}_0 + k_y \mathbf{y}_0$. This is very different from the case of the same refraction at an interface with a double-negative medium where *the normal* component of the wave vector changes sign.

What about the evanescent modes? It can be shown that they are at resonance with the phase conjugating surface so that the strong (theoretically infinite) reflection takes place at the surface, although the field transformation in the sheets (the complex conjugate operation) does not amplify the fields. The details are given in Ref. 8; here we will just try to convince the reader with the following simple physical argument.

Let us consider a single plane-wave component interacting with a single phase conjugating surface in free space. The plane wave is incident from the half space $z < 0$. On both sides of the phase conjugating sheet the tangential fields satisfy the usual relation between the fields in a free-space plane wave (the following equations are valid for TM or TE waves separately):

$$\mathbf{E}_t(k_x, k_y)\Big|_{z=\pm 0} = -Z_{\mathrm{TM,TE}} \, \mathbf{z}_0 \times \mathbf{H}_t(k_x, k_y)\Big|_{z=\pm 0}. \tag{11}$$

Here the free-space wave impedances for TM- and TE-polarized waves read

$$Z_{\mathrm{TM}} = \eta_0 \sqrt{1 - \frac{k_t^2}{k_0^2}}, \qquad Z_{\mathrm{TE}} = \eta_0 \frac{1}{\sqrt{1 - \frac{k_t^2}{k_0^2}}}, \tag{12}$$

where $k_0 = \omega/c$ is the free-space wavenumber, $\eta_0 = \sqrt{\mu_0/\varepsilon_0}$, and $k_t^2 = k_x^2 + k_y^2$. But on the other hand the tangential

fields satisfy also the boundary condition (6). Together with the impedance relation (11) this leads to

$$\mathbf{E}_t(k_x, k_y)\Big|_{z=-0} = \mathbf{E}_t^*(-k_x, -k_y)\Big|_{z=+0}$$
$$= -Z_{\text{TM,TE}}^* \, \mathbf{z}_0 \times \mathbf{H}_t^*(-k_x, -k_y)\Big|_{z=+0}$$
$$= -Z_{\text{TM,TE}}^* \, \mathbf{z}_0 \times \mathbf{H}_t(k_x, k_y)\Big|_{z=-0}. \tag{13}$$

Thus, a wave incident on the sheet from one side "sees" the surface impedance which equals to the complex conjugate of the wave impedance in free space. The reflection coefficient reads

$$R_{\text{TM,TE}} = \frac{Z_{\text{TM,TE}}^* - Z_{\text{TM,TE}}}{Z_{\text{TM,TE}}^* + Z_{\text{TM,TE}}}. \tag{14}$$

If the wave is a propagating wave, that is, $|\mathbf{k}_t| \equiv k_t \equiv \sqrt{k_x^2 + k_y^2} < k_0 \equiv \omega/c$, then its wave impedance is a real number, and the reflection coefficients equal zero. This proves that the propagating modes experience negative refraction without any reflection.

If the wave is evanescent, that is, $k_t \equiv \sqrt{k_x^2 + k_y^2} > k_0$, the wave impedances (11) are purely imaginary and the reflection coefficient is infinite. The transmission coefficient is also infinite due to the boundary condition (5). This is obviously a resonant condition which can be also understood as a condition for existence of a surface mode.[8] Note that this resonant condition holds for all values of the tangential wave number $k_t > k_0$, which is the condition for perfect lensing of all evanescent field components.

The physical reason of such a resonance is rather simple. Consider, for instance, the waves of TM polarization. The characteristic impedance of an evanescent TM wave (12) can be written as $Z_{\text{TM}} = -j\eta_0 \alpha / k_0$, where α is the decay factor: $\alpha = \sqrt{k_t^2 - k_0^2}$. We conclude that a TM evanescent wave has capacitive characteristic impedance. Due to the conjugating interface, the same impedance of the matching TM wave behind the interface (at $z = +0$) is seen as inductive in front of the interface (at $z = -0$), which reminds of a "connection" of two reactances of the opposite character in a parallel oscillatory circuit. Probably, A. Alù and N. Engheta[13] were the first to identify and explain the resonance of the same nature that happens at the border of a double-positive and a double-negative material.

Therefore, when an incident evanescent wave excites a conjugating surface, it resonantly excites a surface mode that matches its transversal propagation factor and this results in very strong (theoretically infinite) reflected and transmitted waves at the surface. The strong reflection was also found to be the key to sub-wavelength imaging in a pair of parametrically pumped nonlinear *nonmagnetic* sheets studied in Ref. 10 The above discussion shows that in a metasurface realizing the boundary conditions (6) the reflection and transmission coefficients for evanescent modes tend to infinity due to a high-quality resonance (theoretically, with an infinite quality factor), while, in Ref. 10, the surface itself parametrically amplifies the fields.

C. Equivalent surface currents on the phase conjugating sheet

One may notice that the boundary conditions (6) imply discontinuity of both tangential electric and magnetic fields across the phase conjugating plane. The jumps of the fields can be expressed as follows:

$$\mathbf{E}_t(x, y)\Big|_{z=+0} - \mathbf{E}_t(x, y)\Big|_{z=-0} = -2j \, \text{Im}[\mathbf{E}_t(x, y)]\Big|_{z=-0}, \tag{15}$$

$$\mathbf{H}_t(x, y)\Big|_{z=+0} - \mathbf{H}_t(x, y)\Big|_{z=-0} = -2j \, \text{Im}[\mathbf{H}_t(x, y)]\Big|_{z=-0}. \tag{16}$$

These jumps are related to the equivalent magnetic and electric surface currents that exist on the surface:

$$\mathbf{z}_0 \times \mathbf{J}_m(x, y) = \mathbf{E}_t(x, y)\Big|_{z=+0} - \mathbf{E}_t(x, y)\Big|_{z=-0}$$
$$= -2j \, \text{Im}[\mathbf{E}_t(x, y)]\Big|_{z=-0} = 2j \, \text{Im}[\mathbf{E}_t(x, y)]\Big|_{z=+0}, \tag{17}$$

$$-\mathbf{z}_0 \times \mathbf{J}_e(x, y) = \mathbf{H}_t(x, y)\Big|_{z=+0} - \mathbf{H}_t(x, y)\Big|_{z=-0}$$
$$= -2j \, \text{Im}[\mathbf{H}_t(x, y)]\Big|_{z=-0} = 2j \, \text{Im}[\mathbf{H}_t(x, y)]\Big|_{z=+0}. \tag{18}$$

Let us stress already at this point that the relations (17)–(18) are the only physical conditions one has to satisfy in a subwavelength imaging device based on phase conjugating sheets. Nothing more is required! Essentially, these relations tell us that it is enough in practice to realize a metasurface that reacts with certain magnetic and electric surface currents to the imaginary parts of the tangential electric and magnetic fields *at a given side* of the surface. This also shows that there is no need for extra-strong pumping or super-efficient nonlinear conversion as in Ref. 10. Moreover, from (17)–(18) we observe that the induced *electric* current should be proportional to the *magnetic* field on the sheet (more precisely, to its imaginary part). Likewise, the induced *magnetic* current is proportional to the *electric* field. This is quite different from the known approaches based on layers of nonlinear dielectrics or magnetics.[10,12]

Let us decompose each of these surface currents into a sum of two currents: $\mathbf{J}_e = \mathbf{J}_e^{(1)} + \mathbf{J}_e^{(2)}$, $\mathbf{J}_m = \mathbf{J}_m^{(1)} + \mathbf{J}_m^{(2)}$, where

$$-\mathbf{z}_0 \times \mathbf{J}_e^{(1)} = -\mathbf{H}_t \Big|_{z=-0} \quad , \quad \mathbf{z}_0 \times \mathbf{J}_m^{(1)} = -\mathbf{E}_t \Big|_{z=-0}, \tag{19}$$

$$-\mathbf{z}_0 \times \mathbf{J}_e^{(2)} = \mathbf{H}_t \Big|_{z=+0} \quad , \quad \mathbf{z}_0 \times \mathbf{J}_m^{(2)} = \mathbf{E}_t \Big|_{z=+0}. \tag{20}$$

One can see that the pair of the surface currents $\mathbf{J}_e^{(1)}$, $\mathbf{J}_m^{(1)}$ is essentially an equivalent Huygens source defined at the plane $z = -0$. In the half-space $z > 0$ this source produces the field which is the negate of the field that the external sources located at $z < 0$ induce in the half-space $z > 0$ (the negation is due to the minus signs in the right-hand side of (19)). Thus, the physical role of the currents $\mathbf{J}_e^{(1)}$, $\mathbf{J}_m^{(1)}$ when concerned with the half-space $z > 0$ is to cancel the field incident from the other half-space. The same holds for the other pair of currents $\mathbf{J}_e^{(2)}$, $\mathbf{J}_m^{(2)}$ when concerned with the half-space $z < 0$. These currents form a Huygens source defined at $z = +0$ plane. In the half-space $z < 0$ they cancel (pay attention to the direction of the normal!) the field produced by the external sources from the $z > 0$ half-space.

From the other hand, the pair of currents $\mathbf{J}_e^{(1)}$, $\mathbf{J}_m^{(1)}$ plays another role when concerned with the half-space $z < 0$. Indeed, using the boundary conditions (6) we write

$$-\mathbf{z}_0 \times \mathbf{J}_e^{(1)} = -\mathbf{H}_t^* \Big|_{z=+0}, \quad \mathbf{z}_0 \times \mathbf{J}_m^{(1)} = -\mathbf{E}_t^* \Big|_{z=+0}, \tag{21}$$

from which it is evident that these currents can be identified also as an equivalent source located at the plane $z = +0$ that produces at $z < 0$ the conjugated field of the sources located in the half-space $z > 0$. Respectively, $\mathbf{J}_e^{(2)}$, $\mathbf{J}_m^{(2)}$ produce the conjugated field in the region $z > 0$.

To summarize, we have identified the following roles of the currents:

- The pair $\mathbf{J}_e^{(1)}$, $\mathbf{J}_m^{(1)}$ cancels the field incident from $z < 0$ to the half-space $z > 0$ and creates the conjugated field of the sources from the half-space $z > 0$ in the half-space $z < 0$;

- The pair $\mathbf{J}_e^{(2)}$, $\mathbf{J}_m^{(2)}$ cancels the field incident from $z > 0$ to the half-space $z < 0$ and creates the conjugated field of the sources from the half-space $z < 0$ in the half-space $z > 0$.

III. PHASE CONJUGATING SURFACE AS AN ARRAY OF BI-ANISOTROPIC NONLINEAR INCLUSIONS

From the above results we see that the ideal phase conjugating surface should respond to the fields with both electric and magnetic polarization. Dependence of the induced electric current on the magnetic field and *vice versa* suggests that the structure should have some magneto-electric coupling. In this section we investigate if it is possible to realize the ideal phase conjugating boundary conditions (6) with a planar array of nonlinear bi-anisotropic particles.

A. General requirements on susceptibilities of inclusions

Let us first find out how the total induced electric and magnetic surface current densities depend on the *incident* electric and magnetic fields in the array plane. To do that, we consider an isolated phase conjugating surface in the field of a *single* TM (or TE) polarized plane electromagnetic wave (propagating or evanescent). Taking into account the conjugating boundary condition (6) we may formally write the total tangential electric and magnetic fields on

both sides of the surface as

$$\mathbf{E}_t(x,y)\Big|_{z=-0} = (1 + R_{\text{TM,TE}})\mathbf{E}_t^{\text{inc}}(x,y)\Big|_{z=0}, \tag{22}$$

$$\mathbf{E}_t(x,y)\Big|_{z=+0} = (1 + R_{\text{TM,TE}}^*)\left(\mathbf{E}_t^{\text{inc}}(x,y)\right)^*\Big|_{z=0}, \tag{23}$$

$$\mathbf{H}_t(x,y)\Big|_{z=-0} = (1 - R_{\text{TM,TE}})\mathbf{H}_t^{\text{inc}}(x,y)\Big|_{z=0}, \tag{24}$$

$$\mathbf{H}_t(x,y)\Big|_{z=+0} = (1 - R_{\text{TM,TE}}^*)\left(\mathbf{H}_t^{\text{inc}}(x,y)\right)^*\Big|_{z=0}, \tag{25}$$

where the reflection coefficients $R_{\text{TM,TE}}$ are given by (14), from which we notice that $R_{\text{TM,TE}}^* = -R_{\text{TM,TE}}$. The above expressions hold for both propagating and evanescent waves incident from the half space $z < 0$.

Therefore, from (17)–(18) and (22)–(25) we obtain

$$-\mathbf{z}_0 \times \mathbf{J}_m(x,y) = 2j\,\text{Im}(\mathbf{E}_t^{\text{inc}}(x,y))\Big|_{z=0} + 2R_{\text{TM,TE}}\,\text{Re}(\mathbf{E}_t^{\text{inc}}(x,y))\Big|_{z=0}, \tag{26}$$

$$\mathbf{z}_0 \times \mathbf{J}_e(x,y) = 2j\,\text{Im}(\mathbf{H}_t^{\text{inc}}(x,y))\Big|_{z=0} - 2R_{\text{TM,TE}}\,\text{Re}(\mathbf{H}_t^{\text{inc}}(x,y))\Big|_{z=0}. \tag{27}$$

The addends on the right-hand side of (26)–(27) that are proportional to the imaginary part of the incident field are relevant for the propagating waves (for these waves $R_{\text{TM,TE}} = 0$), while for the evanescent waves the addends proportional to the real part of the field are of the most importance, because $|R_{\text{TM,TE}}| \to \infty$ for these modes. It is instructive to compare these observations with the discussion in Sec. II C. From (17)–(18) it follows that in terms of the total tangential fields at a given side of the phase conjugating sheet, the conditions for both propagating and evanescent waves are the same: Eqs. (17)–(18) do not distinguish these waves. Physically, this is because the locations where one must *measure* the fields and where one must *create* the surface currents *are not at the same point*, if one wants to approach a design directly suggested by these equations. Indeed, the mathematical form of Eqs. (17)–(18) demands that the field values must be taken at a point slightly displaced off the surface $z = 0$. On the contrary, in an array of particles (considered here as point objects) the equivalent surface currents depend only on the fields *in the array plane* and, as we will see soon, the required reaction to this field happens to be different for the two types of waves.

A related observation is that in a realistic structure, e.g., an array of nonlinear polarizable bi-anisotropic inclusions, it is not the incident field, but the *local* field $\mathbf{E}_t^{\text{loc}}$, $\mathbf{H}_t^{\text{loc}}$, that excites each and every inclusion in the structure. The latter has a contribution from the secondary field of the induced currents. We may therefore write for the signals at the frequency of the incident wave:

$$\mathbf{E}_t^{\text{loc}}(x,y) = \mathbf{E}_t^{\text{inc}}(x,y) + \overline{\overline{\beta}}_{\text{ee}} \cdot \mathbf{J}_e(x,y), \tag{28}$$

$$\mathbf{H}_t^{\text{loc}}(x,y) = \mathbf{H}_t^{\text{inc}}(x,y) + \overline{\overline{\beta}}_{\text{mm}} \cdot \mathbf{J}_m(x,y), \tag{29}$$

where $\overline{\overline{\beta}}_{\text{ee,mm}}$ are the so-called interaction dyadics. For arbitrary distributed currents these dyadics are understood as operators acting on the currents. However, for the following it is enough to consider the currents of the form $\mathbf{J}_{e,m}(x,y) = \mathbf{J}_{\mathbf{k}_t}^{e,m}\exp(-j\mathbf{k}_t \cdot \mathbf{r}) + \mathbf{J}_{-\mathbf{k}_t}^{e,m}\exp(j\mathbf{k}_t \cdot \mathbf{r})$. In this case, in order for (28)–(29) to hold in a simple dyadic sense, the interaction dyadics must satisfy $\overline{\overline{\beta}}_{\text{ee,mm}} \equiv \overline{\overline{\beta}}_{\text{ee,mm}}(\mathbf{k}_t) = \overline{\overline{\beta}}_{\text{ee,mm}}(-\mathbf{k}_t)$, i.e., the lattice (not the particles!) must have a center of symmetry. There are no cross-terms in (28)–(29) because the tangential magnetic (electric) field of an array of tangential electric (magnetic) dipoles vanishes in the plane of the array.

Additionally, the induced electric and magnetic currents must be sensitive to the phase of the external field, because the conjugating boundary reacts differently to the real and imaginary parts of the tangential electric and magnetic fields. Therefore, the inclusions must react differently to the corresponding components of the local fields. Based on the above discussion we may write

$$\mathbf{J}_e = \overline{\overline{\alpha}}_{\text{ee}}^{\text{re}} \cdot \text{Re}(\mathbf{E}_t^{\text{loc}}) + j\overline{\overline{\alpha}}_{\text{ee}}^{\text{im}} \cdot \text{Im}(\mathbf{E}_t^{\text{loc}}) + \overline{\overline{\alpha}}_{\text{em}}^{\text{re}} \cdot \text{Re}(\mathbf{H}_t^{\text{loc}}) + j\overline{\overline{\alpha}}_{\text{em}}^{\text{im}} \cdot \text{Im}(\mathbf{H}_t^{\text{loc}}), \tag{30}$$

$$\mathbf{J}_m = \overline{\overline{\alpha}}_{\text{me}}^{\text{re}} \cdot \text{Re}(\mathbf{E}_t^{\text{loc}}) + j\overline{\overline{\alpha}}_{\text{me}}^{\text{im}} \cdot \text{Im}(\mathbf{E}_t^{\text{loc}}) + \overline{\overline{\alpha}}_{\text{mm}}^{\text{re}} \cdot \text{Re}(\mathbf{H}_t^{\text{loc}}) + j\overline{\overline{\alpha}}_{\text{mm}}^{\text{im}} \cdot \text{Im}(\mathbf{H}_t^{\text{loc}}), \tag{31}$$

where $\overline{\overline{\alpha}}_{\text{ee,mm,me,em}}^{\text{re,im}}$ are the dyadic polarizabilities to the real and imaginary components of the local fields.

Substituting (31)–(30) into (28)–(29) we obtain

$$\mathbf{E}_t^{\text{inc}} = (\overline{\overline{I}}_t - \overline{\overline{\beta}}_{\text{ee}} \cdot \overline{\overline{\alpha}}_{\text{ee}}^{\text{re}}) \cdot \text{Re}(\mathbf{E}_t^{\text{loc}}) + j(\overline{\overline{I}}_t - \overline{\overline{\beta}}_{\text{ee}} \cdot \overline{\overline{\alpha}}_{\text{ee}}^{\text{im}}) \cdot \text{Im}(\mathbf{E}_t^{\text{loc}})$$
$$- \overline{\overline{\beta}}_{\text{ee}} \cdot \overline{\overline{\alpha}}_{\text{em}}^{\text{re}} \cdot \text{Re}(\mathbf{H}_t^{\text{loc}}) - j\overline{\overline{\beta}}_{\text{ee}} \cdot \overline{\overline{\alpha}}_{\text{em}}^{\text{im}} \cdot \text{Im}(\mathbf{H}_t^{\text{loc}}), \tag{32}$$

$$\mathbf{H}_t^{\text{inc}} = (\overline{\overline{I}}_t - \overline{\overline{\beta}}_{\text{mm}} \cdot \overline{\overline{\alpha}}_{\text{mm}}^{\text{re}}) \cdot \text{Re}(\mathbf{H}_t^{\text{loc}}) + j(\overline{\overline{I}}_t - \overline{\overline{\beta}}_{\text{mm}} \cdot \overline{\overline{\alpha}}_{\text{mm}}^{\text{im}}) \cdot \text{Im}(\mathbf{H}_t^{\text{loc}})$$
$$- \overline{\overline{\beta}}_{\text{mm}} \cdot \overline{\overline{\alpha}}_{\text{me}}^{\text{re}} \cdot \text{Re}(\mathbf{E}_t^{\text{loc}}) - j\overline{\overline{\beta}}_{\text{mm}} \cdot \overline{\overline{\alpha}}_{\text{me}}^{\text{im}} \cdot \text{Im}(\mathbf{E}_t^{\text{loc}}), \quad (33)$$

where $\overline{\overline{I}}_t$ is the unit dyadic in the plane of the array. Respectively,

$$\text{Re}(\mathbf{E}_t^{\text{inc}}) = \text{Re}(\overline{\overline{I}}_t - \overline{\overline{\beta}}_{\text{ee}} \cdot \overline{\overline{\alpha}}_{\text{ee}}^{\text{re}}) \cdot \text{Re}(\mathbf{E}_t^{\text{loc}}) + \text{Im}(\overline{\overline{\beta}}_{\text{ee}} \cdot \overline{\overline{\alpha}}_{\text{ee}}^{\text{im}}) \cdot \text{Im}(\mathbf{E}_t^{\text{loc}})$$
$$- \text{Re}(\overline{\overline{\beta}}_{\text{ee}} \cdot \overline{\overline{\alpha}}_{\text{em}}^{\text{re}}) \cdot \text{Re}(\mathbf{H}_t^{\text{loc}}) + \text{Im}(\overline{\overline{\beta}}_{\text{ee}} \cdot \overline{\overline{\alpha}}_{\text{em}}^{\text{im}}) \cdot \text{Im}(\mathbf{H}_t^{\text{loc}}), \quad (34)$$

$$\text{Im}(\mathbf{E}_t^{\text{inc}}) = - \text{Im}(\overline{\overline{\beta}}_{\text{ee}} \cdot \overline{\overline{\alpha}}_{\text{ee}}^{\text{re}}) \cdot \text{Re}(\mathbf{E}_t^{\text{loc}}) + \text{Re}(\overline{\overline{I}}_t - \overline{\overline{\beta}}_{\text{ee}} \cdot \overline{\overline{\alpha}}_{\text{ee}}^{\text{im}}) \cdot \text{Im}(\mathbf{E}_t^{\text{loc}})$$
$$- \text{Im}(\overline{\overline{\beta}}_{\text{ee}} \cdot \overline{\overline{\alpha}}_{\text{em}}^{\text{re}}) \cdot \text{Re}(\mathbf{H}_t^{\text{loc}}) - \text{Re}(\overline{\overline{\beta}}_{\text{ee}} \cdot \overline{\overline{\alpha}}_{\text{em}}^{\text{im}}) \cdot \text{Im}(\mathbf{H}_t^{\text{loc}}), \quad (35)$$

$$\text{Re}(\mathbf{H}_t^{\text{inc}}) = \text{Re}(\overline{\overline{I}}_t - \overline{\overline{\beta}}_{\text{mm}} \cdot \overline{\overline{\alpha}}_{\text{mm}}^{\text{re}}) \cdot \text{Re}(\mathbf{H}_t^{\text{loc}}) + \text{Im}(\overline{\overline{\beta}}_{\text{mm}} \cdot \overline{\overline{\alpha}}_{\text{mm}}^{\text{im}}) \cdot \text{Im}(\mathbf{H}_t^{\text{loc}})$$
$$- \text{Re}(\overline{\overline{\beta}}_{\text{mm}} \cdot \overline{\overline{\alpha}}_{\text{me}}^{\text{re}}) \cdot \text{Re}(\mathbf{E}_t^{\text{loc}}) + \text{Im}(\overline{\overline{\beta}}_{\text{mm}} \cdot \overline{\overline{\alpha}}_{\text{me}}^{\text{im}}) \cdot \text{Im}(\mathbf{E}_t^{\text{loc}}), \quad (36)$$

$$\text{Im}(\mathbf{H}_t^{\text{inc}}) = - \text{Im}(\overline{\overline{\beta}}_{\text{mm}} \cdot \overline{\overline{\alpha}}_{\text{mm}}^{\text{re}}) \cdot \text{Re}(\mathbf{H}_t^{\text{loc}}) + \text{Re}(\overline{\overline{I}}_t - \overline{\overline{\beta}}_{\text{mm}} \cdot \overline{\overline{\alpha}}_{\text{mm}}^{\text{im}}) \cdot \text{Im}(\mathbf{H}_t^{\text{loc}})$$
$$- \text{Im}(\overline{\overline{\beta}}_{\text{mm}} \cdot \overline{\overline{\alpha}}_{\text{me}}^{\text{re}}) \cdot \text{Re}(\mathbf{E}_t^{\text{loc}}) - \text{Re}(\overline{\overline{\beta}}_{\text{mm}} \cdot \overline{\overline{\alpha}}_{\text{me}}^{\text{im}}) \cdot \text{Im}(\mathbf{E}_t^{\text{loc}}). \quad (37)$$

These expressions can be substituted into (26)–(27) from which one obtains a set of dyadic relations for the polarizabilities assuming that the four components of the local fields $\text{Re}(\mathbf{E}_t^{\text{loc}}(x,y))$, $\text{Re}(\mathbf{H}_t^{\text{loc}}(x,y))$, $\text{Im}(\mathbf{E}_t^{\text{loc}}(x,y))$, and $\text{Im}(\mathbf{H}_t^{\text{loc}}(x,y))$ are independent. Doing so we obtain the following relations:

$$\mathbf{z}_0 \times \overline{\overline{\alpha}}_{\text{me}}^{\text{re}} = 2j \, \text{Im}(\overline{\overline{\beta}}_{\text{ee}} \cdot \overline{\overline{\alpha}}_{\text{ee}}^{\text{re}}) - 2\overline{\overline{R}} \cdot \text{Re}(\overline{\overline{I}}_t - \overline{\overline{\beta}}_{\text{ee}} \cdot \overline{\overline{\alpha}}_{\text{ee}}^{\text{re}}), \tag{38}$$

$$j\mathbf{z}_0 \times \overline{\overline{\alpha}}_{\text{me}}^{\text{im}} = -2j \, \text{Re}(\overline{\overline{I}}_t - \overline{\overline{\beta}}_{\text{ee}} \cdot \overline{\overline{\alpha}}_{\text{ee}}^{\text{im}}) - 2\overline{\overline{R}} \cdot \text{Im}(\overline{\overline{\beta}}_{\text{ee}} \cdot \overline{\overline{\alpha}}_{\text{ee}}^{\text{im}}), \tag{39}$$

$$\mathbf{z}_0 \times \overline{\overline{\alpha}}_{\text{mm}}^{\text{re}} = 2j \, \text{Im}(\overline{\overline{\beta}}_{\text{ee}} \cdot \overline{\overline{\alpha}}_{\text{em}}^{\text{re}}) + 2\overline{\overline{R}} \cdot \text{Re}(\overline{\overline{\beta}}_{\text{ee}} \cdot \overline{\overline{\alpha}}_{\text{em}}^{\text{re}}), \tag{40}$$

$$j\mathbf{z}_0 \times \overline{\overline{\alpha}}_{\text{mm}}^{\text{im}} = 2j \, \text{Re}(\overline{\overline{\beta}}_{\text{ee}} \cdot \overline{\overline{\alpha}}_{\text{em}}^{\text{im}}) - 2\overline{\overline{R}} \cdot \text{Im}(\overline{\overline{\beta}}_{\text{ee}} \cdot \overline{\overline{\alpha}}_{\text{em}}^{\text{im}}), \tag{41}$$

$$\mathbf{z}_0 \times \overline{\overline{\alpha}}_{\text{ee}}^{\text{re}} = -2j \, \text{Im}(\overline{\overline{\beta}}_{\text{mm}} \cdot \overline{\overline{\alpha}}_{\text{me}}^{\text{re}}) + 2\overline{\overline{R}} \cdot \text{Re}(\overline{\overline{\beta}}_{\text{mm}} \cdot \overline{\overline{\alpha}}_{\text{me}}^{\text{re}}), \tag{42}$$

$$j\mathbf{z}_0 \times \overline{\overline{\alpha}}_{\text{ee}}^{\text{im}} = -2j \, \text{Re}(\overline{\overline{\beta}}_{\text{mm}} \cdot \overline{\overline{\alpha}}_{\text{me}}^{\text{im}}) - 2\overline{\overline{R}} \cdot \text{Im}(\overline{\overline{\beta}}_{\text{mm}} \cdot \overline{\overline{\alpha}}_{\text{me}}^{\text{im}}), \tag{43}$$

$$\mathbf{z}_0 \times \overline{\overline{\alpha}}_{\text{em}}^{\text{re}} = -2j \, \text{Im}(\overline{\overline{\beta}}_{\text{mm}} \cdot \overline{\overline{\alpha}}_{\text{mm}}^{\text{re}}) - 2\overline{\overline{R}} \cdot \text{Re}(\overline{\overline{I}}_t - \overline{\overline{\beta}}_{\text{mm}} \cdot \overline{\overline{\alpha}}_{\text{mm}}^{\text{re}}), \tag{44}$$

$$j\mathbf{z}_0 \times \overline{\overline{\alpha}}_{\text{em}}^{\text{im}} = 2j \, \text{Re}(\overline{\overline{I}}_t - \overline{\overline{\beta}}_{\text{mm}} \cdot \overline{\overline{\alpha}}_{\text{mm}}^{\text{im}}) - 2\overline{\overline{R}} \cdot \text{Im}(\overline{\overline{\beta}}_{\text{mm}} \cdot \overline{\overline{\alpha}}_{\text{mm}}^{\text{im}}), \tag{45}$$

where $\overline{\overline{R}}$ is the dyadic reflection coefficient defined in terms of $R_{\text{TM,TE}}$ as

$$\overline{\overline{R}} = R_{\text{TE}} \frac{\mathbf{z}_0 \mathbf{z}_0 \overset{\times}{\times} \mathbf{k}_t \mathbf{k}_t}{k_t^2} + R_{\text{TM}} \frac{\mathbf{k}_t \mathbf{k}_t}{k_t^2} \tag{46}$$

(for the definition of the double cross product and other dyadic algebra rules see, e.g., Ref. 14). One may notice that because $\overline{\overline{R}}$ in the above relations is either zero or purely imaginary: $(\overline{\overline{R}})^* = -\overline{\overline{R}}$, it follows that $\text{Re}(\overline{\overline{\alpha}}_{\text{ee,mm,em,me}}^{\text{re}}) = \text{Im}(\overline{\overline{\alpha}}_{\text{ee,mm,em,me}}^{\text{im}}) = 0$. Therefore, the equations (38)–(45) can be also written as

$$\mathbf{z}_0 \times \overline{\overline{\alpha}}_{\text{me}}^{\text{re}} = 2 \left[\text{Re}(\overline{\overline{\beta}}_{\text{ee}}) + j\overline{\overline{R}} \cdot \text{Im}(\overline{\overline{\beta}}_{\text{ee}}) \right] \cdot \overline{\overline{\alpha}}_{\text{ee}}^{\text{re}} - 2\overline{\overline{R}}, \tag{47}$$

$$\mathbf{z}_0 \times \overline{\overline{\alpha}}_{\text{me}}^{\text{im}} = 2 \left[\text{Re}(\overline{\overline{\beta}}_{\text{ee}}) + j\overline{\overline{R}} \cdot \text{Im}(\overline{\overline{\beta}}_{\text{ee}}) \right] \cdot \overline{\overline{\alpha}}_{\text{ee}}^{\text{im}} - 2\overline{\overline{I}}_t, \tag{48}$$

$$\mathbf{z}_0 \times \overline{\overline{\alpha}}_{\text{mm}}^{\text{re}} = 2 \left[\text{Re}(\overline{\overline{\beta}}_{\text{ee}}) + j\overline{\overline{R}} \cdot \text{Im}(\overline{\overline{\beta}}_{\text{ee}}) \right] \cdot \overline{\overline{\alpha}}_{\text{em}}^{\text{re}}, \tag{49}$$

$$\mathbf{z}_0 \times \overline{\overline{\alpha}}_{\text{mm}}^{\text{im}} = 2 \left[\text{Re}(\overline{\overline{\beta}}_{\text{ee}}) + j\overline{\overline{R}} \cdot \text{Im}(\overline{\overline{\beta}}_{\text{ee}}) \right] \cdot \overline{\overline{\alpha}}_{\text{em}}^{\text{im}}, \tag{50}$$

$$\mathbf{z}_0 \times \overline{\overline{\alpha}}^{\mathrm{re}}_{\mathrm{ee}} = -2\left[\mathrm{Re}(\overline{\overline{\beta}}_{\mathrm{mm}}) - j\overline{\overline{R}} \cdot \mathrm{Im}(\overline{\overline{\beta}}_{\mathrm{mm}})\right] \cdot \overline{\overline{\alpha}}^{\mathrm{re}}_{\mathrm{me}}, \tag{51}$$

$$\mathbf{z}_0 \times \overline{\overline{\alpha}}^{\mathrm{im}}_{\mathrm{ee}} = -2\left[\mathrm{Re}(\overline{\overline{\beta}}_{\mathrm{mm}}) - j\overline{\overline{R}} \cdot \mathrm{Im}(\overline{\overline{\beta}}_{\mathrm{mm}})\right] \cdot \overline{\overline{\alpha}}^{\mathrm{im}}_{\mathrm{me}}, \tag{52}$$

$$\mathbf{z}_0 \times \overline{\overline{\alpha}}^{\mathrm{re}}_{\mathrm{em}} = -2\left[\mathrm{Re}(\overline{\overline{\beta}}_{\mathrm{mm}}) - j\overline{\overline{R}} \cdot \mathrm{Im}(\overline{\overline{\beta}}_{\mathrm{mm}})\right] \cdot \overline{\overline{\alpha}}^{\mathrm{re}}_{\mathrm{mm}} - 2\overline{\overline{R}}, \tag{53}$$

$$\mathbf{z}_0 \times \overline{\overline{\alpha}}^{\mathrm{im}}_{\mathrm{em}} = -2\left[\mathrm{Re}(\overline{\overline{\beta}}_{\mathrm{mm}}) - j\overline{\overline{R}} \cdot \mathrm{Im}(\overline{\overline{\beta}}_{\mathrm{mm}})\right] \cdot \overline{\overline{\alpha}}^{\mathrm{im}}_{\mathrm{mm}} + 2\overline{\overline{I}}_{\mathrm{t}}. \tag{54}$$

Let us consider first the propagating part of the spectrum. For such waves, $\overline{\overline{R}} = 0$, and the above relations simplify. Also, we can write $\overline{\overline{\beta}}_{\mathrm{ee}} = \eta_0 \overline{\overline{\beta}}$, and $\overline{\overline{\beta}}_{\mathrm{mm}} = \eta_0^{-1} \overline{\overline{\beta}}$, where $\overline{\overline{\beta}}$ is the dimensionless interaction dyadic which, by duality, is the same for the electric and magnetic currents as they are due to the electric and magnetic dipole moments that belong to the same particles in the array. The solution of the system of dyadic equations (47)–(54) in the case of $\overline{\overline{R}} = 0$ is

$$\overline{\overline{\alpha}}^{\mathrm{re}}_{\mathrm{ee,mm,em,me}} = 0, \tag{55}$$

$$\overline{\overline{\alpha}}^{\mathrm{im}}_{\mathrm{me}} = -\overline{\overline{\alpha}}^{\mathrm{im}}_{\mathrm{em}} = 2\left[\overline{\overline{I}}_{\mathrm{t}} + 4\left(\mathbf{z}_0 \times \mathrm{Re}(\overline{\overline{\beta}})\right)^2\right]^{-1} \cdot (\mathbf{z}_0 \times \overline{\overline{I}}_{\mathrm{t}}), \tag{56}$$

$$\eta_0 \overline{\overline{\alpha}}^{\mathrm{im}}_{\mathrm{ee}} = \eta_0^{-1} \overline{\overline{\alpha}}^{\mathrm{im}}_{\mathrm{mm}} = 4\mathbf{z}_0 \times \mathrm{Re}(\overline{\overline{\beta}}) \cdot \left[\overline{\overline{I}}_{\mathrm{t}} + 4\left(\mathbf{z}_0 \times \mathrm{Re}(\overline{\overline{\beta}})\right)^2\right]^{-1} \cdot (\mathbf{z}_0 \times \overline{\overline{I}}_{\mathrm{t}}). \tag{57}$$

It can be shown[15,16] that the real part of the interaction dyadic $\overline{\overline{\beta}}$ for a planar array verifies

$$\mathrm{Re}(\overline{\overline{\beta}}) = -\frac{1}{2\cos\theta} \frac{\mathbf{z}_0 \mathbf{z}_0 \overset{\times}{\times} \mathbf{k}_{\mathrm{t}}\mathbf{k}_{\mathrm{t}}}{k_{\mathrm{t}}^2} - \frac{\cos\theta}{2} \frac{\mathbf{k}_{\mathrm{t}}\mathbf{k}_{\mathrm{t}}}{k_{\mathrm{t}}^2} + \frac{k_0^2 A_0}{6\pi} \overline{\overline{I}}_{\mathrm{t}}, \tag{58}$$

where θ is the angle of incidence: $\cos\theta = \sqrt{1 - k_{\mathrm{t}}^2/k_0^2}$, and A_0 is the unit cell area. This result holds for arrays with arbitrary unit cell geometries, provided that the arrays do not produce higher-order diffraction lobes.

It is quite interesting that the imaginary part of the interaction constant that contains the information about the microstructure of the array has completely disappeared from the above solution. The imaginary part of the interaction constant does not contribute in this case because the induced currents $\mathbf{J}_{\mathrm{e}}$ and $\mathbf{J}_{\mathrm{m}}$ are always imaginary, and the respective additions to the interaction field $j\,\mathrm{Im}(\overline{\overline{\beta}}_{\mathrm{ee}}) \cdot \mathbf{J}_{\mathrm{e}}$ and $j\,\mathrm{Im}(\overline{\overline{\beta}}_{\mathrm{mm}}) \cdot \mathbf{J}_{\mathrm{m}}$ are real-valued, to which the particles do not react. Thus, the interaction of the particles in the array is irrelevant in the considered case, and each particle radiates effectively as in free space.

We may substitute (58) into (56)–(57), taking into account that

$$\left(\mathbf{z}_0 \times \mathrm{Re}(\overline{\overline{\beta}})\right)^2 = \left[-\frac{1}{4} - \left(\frac{k_0^2 A_0}{6\pi}\right)^2 + \frac{k_0^2 A_0}{12\pi}\left(\cos\theta + \frac{1}{\cos\theta}\right)\right]\overline{\overline{I}}_{\mathrm{t}}, \tag{59}$$

and obtain

$$\overline{\overline{\alpha}}^{\mathrm{im}}_{\mathrm{me}} = -\overline{\overline{\alpha}}^{\mathrm{im}}_{\mathrm{em}} = \frac{6\pi}{k_0^2 A_0}\left(\cos\theta + \frac{1}{\cos\theta} - \frac{k_0^2 A_0}{3\pi}\right)^{-1}(\mathbf{z}_0 \times \overline{\overline{I}}_{\mathrm{t}}), \tag{60}$$

$$\eta_0 \overline{\overline{\alpha}}^{\mathrm{im}}_{\mathrm{ee}} = \eta_0^{-1} \overline{\overline{\alpha}}^{\mathrm{im}}_{\mathrm{mm}} = -\frac{12\pi}{k_0^2 A_0}\left(\cos\theta + \frac{1}{\cos\theta} - \frac{k_0^2 A_0}{3\pi}\right)^{-1}(\mathbf{z}_0 \mathbf{z}_0 \overset{\times}{\times} \mathrm{Re}(\overline{\overline{\beta}})). \tag{61}$$

For practical purposes, considering the phase conjugation of paraxial beams in dense arrays, we may approximate the above relations as

$$\overline{\overline{\alpha}}^{\mathrm{im}}_{\mathrm{me}} = -\overline{\overline{\alpha}}^{\mathrm{im}}_{\mathrm{em}} \approx \frac{3\pi}{k_0^2 A_0}(\mathbf{z}_0 \times \overline{\overline{I}}_{\mathrm{t}}), \tag{62}$$

$$\eta_0 \overline{\overline{\alpha}}^{\mathrm{im}}_{\mathrm{ee}} = \eta_0^{-1} \overline{\overline{\alpha}}^{\mathrm{im}}_{\mathrm{mm}} \approx \frac{3\pi}{k_0^2 A_0}\overline{\overline{I}}_{\mathrm{t}}. \tag{63}$$

Because of the form of the relations (22)–(25), the obtained exact solutions (56)–(57) and their approximations (62)–(63) are valid for arbitrary plane waves incident from the half space $z < 0$. The solution for the case of incidence from the half space $z > 0$ is obtained by replacing $\mathbf{z}_0$ with $-\mathbf{z}_0$ in (56)–(57) and (62)–(63), which changes signs of $\overline{\overline{\alpha}}^{\mathrm{im}}_{\mathrm{em,me}}$.

From the above results we see that the particle must be "invisible" for the real-valued electric and magnetic fields, while the polarizabilities of the particle to the imaginary-valued fields must be such that the electric and magnetic currents form Huygens pairs that absorb the incident wave and produce the phase conjugated wave.

For the evanescent waves $|R_{\mathrm{TM,TE}}| \to \infty$, therefore, it is convenient to multiply the equations (47)–(54) by $\overline{\overline{R}}^{-1}$ from the left. Then, in the limit $\overline{\overline{R}}^{-1} \to 0$ the following solution of the system (47)–(54) can be immediately found:

$$\eta_0 \overline{\overline{\alpha}}_{\mathrm{ee}}^{\mathrm{re}} = \eta_0^{-1} \overline{\overline{\alpha}}_{\mathrm{mm}}^{\mathrm{re}} = -j \left[\mathrm{Im}(\overline{\overline{\beta}}) \right]^{-1}, \tag{64}$$

$$\overline{\overline{\alpha}}_{\mathrm{ee,mm}}^{\mathrm{im}} = \overline{\overline{\alpha}}_{\mathrm{em,me}}^{\mathrm{re,im}} = 0. \tag{65}$$

The same solution can be also obtained with a more accurate treatment. Let us introduce the notations $\overline{\overline{C}}_{\mathrm{e}} = \mathrm{Re}(\overline{\overline{\beta}}_{\mathrm{ee}}) + j\overline{\overline{R}} \cdot \mathrm{Im}(\overline{\overline{\beta}}_{\mathrm{ee}})$ and $\overline{\overline{C}}_{\mathrm{m}} = \mathrm{Re}(\overline{\overline{\beta}}_{\mathrm{mm}}) - j\overline{\overline{R}} \cdot \mathrm{Im}(\overline{\overline{\beta}}_{\mathrm{mm}})$. Then, in these notations, we may, for example, write the solution for $\overline{\overline{\alpha}}_{\mathrm{ee}}^{\mathrm{re}}$ as

$$\overline{\overline{\alpha}}_{\mathrm{ee}}^{\mathrm{re}} = 4 \left[\overline{\overline{I}}_{\mathrm{t}} + 4(\mathbf{z}_0 \times \overline{\overline{C}}_{\mathrm{m}}) \cdot (\mathbf{z}_0 \times \overline{\overline{C}}_{\mathrm{e}}) \right]^{-1} \cdot (\mathbf{z}_0 \times \overline{\overline{C}}_{\mathrm{m}}) \cdot (\mathbf{z}_0 \times \overline{\overline{R}})$$

$$= \left[\overline{\overline{I}}_{\mathrm{t}} + \frac{1}{4}(\mathbf{z}_0 \times \overline{\overline{C}}_{\mathrm{e}})^{-1} \cdot (\mathbf{z}_0 \times \overline{\overline{C}}_{\mathrm{m}})^{-1} \right]^{-1} \cdot (\mathbf{z}_0 \times \overline{\overline{C}}_{\mathrm{e}})^{-1} \cdot (\mathbf{z}_0 \times \overline{\overline{R}})$$

$$= \overline{\overline{C}}_{\mathrm{e}}^{-1} \cdot \overline{\overline{R}} + \mathcal{O}(\overline{\overline{R}}^{-2}). \tag{66}$$

Next,

$$\overline{\overline{C}}_{\mathrm{e}}^{-1} \cdot \overline{\overline{R}} = -j \left[\mathrm{Im}(\overline{\overline{\beta}}_{\mathrm{ee}}) \right]^{-1} \cdot \left[\overline{\overline{I}}_{\mathrm{t}} - j\overline{\overline{R}}^{-1} \cdot \mathrm{Re}(\overline{\overline{\beta}}_{\mathrm{ee}}) \cdot \left(\mathrm{Im}(\overline{\overline{\beta}}_{\mathrm{ee}}) \right)^{-1} \right]^{-1}$$

$$= -j \left[\mathrm{Im}(\overline{\overline{\beta}}_{\mathrm{ee}}) \right]^{-1} + \mathcal{O}(\overline{\overline{R}}^{-1}), \tag{67}$$

which leads to (64).

From (64)–(65) we conclude that to conjugate the evanescent part of the spectrum the inclusions must be "invisible" to the imaginary part of the electric and magnetic fields. The inclusions do not have to be bi-anisotropic in this case. The particles are purely reactive and their reactance should compensate the reactance due to particle interactions, creating a resonant structure.

From a physical point of view, condition (64) can be understood as a condition for a surface polariton resonance at the array surface. Indeed, for particles with the polarizabilities (64)–(65) we may write $\mathbf{J}_{\mathrm{e}} = \overline{\overline{\alpha}}_{\mathrm{ee}}^{\mathrm{re}} \cdot \mathrm{Re}(\mathbf{E}^{\mathrm{loc}})$. From the other hand, $\mathbf{E}^{\mathrm{loc}} = \mathbf{E}^{\mathrm{inc}} + \overline{\overline{\beta}}_{\mathrm{ee}} \cdot \mathbf{J}_{\mathrm{e}}$. Therefore,

$$\mathbf{J}_{\mathrm{e}} = \overline{\overline{\alpha}}_{\mathrm{ee}}^{\mathrm{re}} \cdot \mathrm{Re}(\mathbf{E}^{\mathrm{inc}} + \overline{\overline{\beta}}_{\mathrm{ee}} \cdot \mathbf{J}_{\mathrm{e}}) = \overline{\overline{\alpha}}_{\mathrm{ee}}^{\mathrm{re}} \cdot \mathrm{Re}(\mathbf{E}^{\mathrm{inc}}) + j\overline{\overline{\alpha}}_{\mathrm{ee}}^{\mathrm{re}} \cdot \mathrm{Im}(\overline{\overline{\beta}}_{\mathrm{ee}}) \cdot \mathbf{J}_{\mathrm{e}}, \tag{68}$$

because both $\overline{\overline{\alpha}}_{\mathrm{ee}}^{\mathrm{re}}$ and $\mathbf{J}_{\mathrm{e}}$ are purely imaginary. From here

$$\mathbf{J}_{\mathrm{e}} = \left[\overline{\overline{I}}_{\mathrm{t}} - j\overline{\overline{\alpha}}_{\mathrm{ee}}^{\mathrm{re}} \cdot \mathrm{Im}(\overline{\overline{\beta}}_{\mathrm{ee}}) \right]^{-1} \cdot \overline{\overline{\alpha}}_{\mathrm{ee}}^{\mathrm{re}} \cdot \mathrm{Re}(\mathbf{E}^{\mathrm{inc}}), \tag{69}$$

and we see that $\mathbf{J}_{\mathrm{e}} \to \infty$ when condition (64) is fulfilled. A similar resonance is responsible for the enhancement of the evanescent waves in a pair of linear plasmon-polariton resonant grids studied in previous works.[3–6]

B. Electromagnetic properties of the particles forming phase conjugating sheets

Although the principle of operation of the field-conjugating perfect lens is the nonlinear operation of complex conjugation of electromagnetic fields, it is interesting to observe that the particles which perform this operation are characterized by linear polarizabilities with respect to the *real or imaginary parts* of the fields. The nonlinear nature of the particles is thus only in their selective sensitivity to either real or imaginary parts of the complex amplitude of the local fields.

Considering the particle response to the real or imaginary field components separately, we may apply the theory of usual linear bi-anisotropic particles. For the particles which react to the imaginary parts of the field (the particles

excited by the propagating part of the spatial spectrum), we rewrite relations (30), (31), and (62) in terms of the induced electric and magnetic dipole moments of individual particles $\mathbf{p}_{e,m}$ and the local fields:

$$\mathbf{p}_e = \left(-j\frac{3\pi\epsilon_0}{k_0^3}\right) j\,\mathrm{Im}(\mathbf{E}_t^{loc}) + \eta_0\left(j\frac{3\pi\epsilon_0}{k_0^3}\right)\mathbf{z}_0 \times j\,\mathrm{Im}(\mathbf{H}_t^{loc})$$

$$= \bar{\bar{a}}_{ee} \cdot j\,\mathrm{Im}(\mathbf{E}_t^{loc}) + \eta_0\bar{\bar{a}}_{em} \cdot j\,\mathrm{Im}(\mathbf{H}_t^{loc}), \tag{70}$$

$$\mathbf{p}_m = \left(-j\frac{3\pi\mu_0}{k_0^3}\right) j\,\mathrm{Im}(\mathbf{H}_t^{loc}) - \frac{1}{\eta_0}\left(j\frac{3\pi\mu_0}{k_0^3}\right)\mathbf{z}_0 \times j\,\mathrm{Im}(\mathbf{E}_t^{loc})$$

$$= \bar{\bar{a}}_{mm} \cdot j\,\mathrm{Im}(\mathbf{H}_t^{loc}) + \frac{1}{\eta_0}\bar{\bar{a}}_{me} \cdot j\,\mathrm{Im}(\mathbf{E}_t^{loc}) \tag{71}$$

(the surface current densities are related to the dipole moments of individual particles as $\mathbf{J}_{e,m} = j\omega\mathbf{p}_{e,m}/A_0$).

These relations show that the particles reacting to the propagating part of the spectrum are bi-anisotropic and nonreciprocal. The magnetoelectric coupling is due to nonreciprocity only (no magnetoelectric coupling due to reciprocal spatial dispersion effects), because the coupling dyadics satisfy

$$\bar{\bar{a}}_{em} = \bar{\bar{a}}_{me}^T. \tag{72}$$

Furthermore, because these dyadics are antisymmetric ($\bar{\bar{a}}_{em} = -\bar{\bar{a}}_{em}^T$, $\bar{\bar{a}}_{me} = -\bar{\bar{a}}_{me}^T$), materials formed by particles of this type belong to the class of moving media.[17,18]

The polarizabilities of lossless bi-anisotropic particles satisfy the following conditions (e.g., Ref. 18):

$$\bar{\bar{a}}_{ee} = \bar{\bar{a}}_{ee}^\dagger, \quad \bar{\bar{a}}_{mm} = \bar{\bar{a}}_{mm}^\dagger, \quad \bar{\bar{a}}_{em} = \bar{\bar{a}}_{me}^\dagger, \tag{73}$$

where $\dagger$ denotes the Hermitian conjugation operation. Obviously, the inclusions with the polarizabilities (70) and (71) have the opposite property of being purely passive or active (there is no stored electromagnetic energy in their near fields), because they satisfy the opposite conditions:

$$\bar{\bar{a}}_{ee} = -\bar{\bar{a}}_{ee}^\dagger, \quad \bar{\bar{a}}_{mm} = -\bar{\bar{a}}_{mm}^\dagger, \quad \bar{\bar{a}}_{em} = -\bar{\bar{a}}_{me}^\dagger. \tag{74}$$

The power extracted from the local fields by one pair of the particles reads

$$P = \frac{1}{2}\mathrm{Re}\{\mathbf{J}_e^* \cdot \mathbf{E}^{loc} + \mathbf{J}_m^* \cdot \mathbf{H}^{loc}\}A_0. \tag{75}$$

Assuming paraxial wave propagation, we can use the polarizability expressions (62) and (63) and assume that the electric and magnetic local fields are related by the free-space wave impedance η_0. In this approximation we find, for the case of plane wave incidence from the half space $z < 0$,

$$P = \frac{1}{2}\frac{3\pi}{k_0^2}\frac{4}{\eta_0}[\mathrm{Im}(E^{loc})]^2 = \frac{6\pi}{k_0^2\eta_0}[\mathrm{Im}(E^{loc})]^2 = \frac{6\pi\eta_0}{k_0^2}[\mathrm{Im}(H^{loc})]^2. \tag{76}$$

As is clear from this result, each of the polarizability components in (62) and (63) brings equal contributions to the extracted power. Noting that the induced dipole moments of ideal absorption-free dipole scatters read (at the resonance)

$$\mathbf{p}_{e0} = \left(-j\frac{6\pi\epsilon_0}{k_0^3}\right)\mathbf{E}^{loc}, \qquad \mathbf{p}_{m0} = \left(-j\frac{6\pi\mu_0}{k_0^3}\right)\mathbf{H}^{loc}, \tag{77}$$

we see that a pair of such ideal dipoles would extract from the fields exactly the same amount of power as our phase conjugating particles (when the complex amplitude of the local field is purely imaginary at the point of the particle). Thus, we can conclude that the particles described by (62) and (63) actually do not absorb power. They act as ideal absorption-free particles, which receive power from the incident field and re-radiate the same amount of power, creating phase conjugated waves of the same intensity as the incident propagating waves.

It is easy to check that the same particles with the polarizabilities (70)–(71) do not react to the plane waves incident from the half space $z > 0$. Indeed, the sign of the magnetic field in these waves is opposite, therefore, the contributions due to $\mathbf{E}^{loc}$ and $\mathbf{H}^{loc}$ to the electric dipole moment $\mathbf{p}_e$ and the magnetic dipole moment $\mathbf{p}_m$ compensate each other in Eqs. (70)–(71), so that $\mathbf{p}_e = \mathbf{p}_m = 0$ under such excitation. As was mentioned in Section III A, to conjugate the waves incident from the half space $z > 0$, one must change the signs of the magnetoelectric coupling terms in (70)–(71). Physically, this requires another array of inclusions with slightly different topology (more details in the next section). Fortunately, the particles in the two arrays do not interact, so that in practice it is possible to combine the two types of particles in a single plane, for example, in a chess board-like structure.

IV. DESIGN OF THE PHASE CONJUGATING BI-ANISOTROPIC INCLUSIONS AT MICROWAVES

A. Case of propagating waves

To approach the design of nonlinear phase conjugating inclusions at microwaves one may start from the ideas behind the well-known omega particle.[19;20] An omega particle is a combination of a short dipole antenna and a small loop antenna. The particle is planar, so that both the dipole and the loop may be printed on a single side of a printed-circuit board. In the most common variant of this linear and reciprocal inclusion the dipole is directly connected to the loop. The nonlinearity and nonreciprocity, thus, can be achieved if one inserts a nonlinear and nonreciprocal four-pole network between the two antennas.

To identify what kind of network one may need, let us first briefly analyze how the linear omega particle reacts to the local electric and magnetic fields. We consider the case when the particle lies in the xz-plane with the dipole antenna oriented along the x-axis. In this geometry, the dipole reacts to the x-component of the electric field, E_x^{loc}, and the loop reacts to the y-component of the magnetic field, H_y^{loc}.

The electromotive force (EMF) induced by the local field in the dipole can be written as

$$\mathcal{E}_{\mathrm{dip}} = h_{\mathrm{dip}} E_x^{\mathrm{loc}}, \tag{78}$$

where h_{dip} is the effective height of the dipole antenna. For a short dipole of the total length $2l$, the effective height is $h_{\mathrm{dip}} = l$. Respectively, the EMF induced in the loop by the magnetic field reads

$$\mathcal{E}_{\mathrm{loop}} = -j\omega\mu_0 S H_y^{\mathrm{loc}}, \tag{79}$$

where $S = \pi r^2$ is the area of the loop. Under a normal plane wave incidence, $H_y^{\mathrm{loc}} = \pm E_x^{\mathrm{loc}}/\eta_0$ (the two signs are for the two possible directions of incidence), therefore,

$$\mathcal{E}_{\mathrm{loop}} = \mp j(k_0 S) E_x^{\mathrm{loc}} = \mp j h_{\mathrm{loop}} E_x^{\mathrm{loc}}, \tag{80}$$

where we have introduced the effective height of a small loop antenna $h_{\mathrm{loop}} = k_0 S$. One may notice that the EMF induced in the loop is in quadrature with respect to the EMF in the dipole. Therefore, when the two antennas are directly connected, these EMFs add up, but never fully compensate (or fully complement) each other. In fact, in the most interesting case when $h_{\mathrm{loop}} = h_{\mathrm{dip}} = l$, the total EMF induced in the antennas is

$$\mathcal{E}_{\mathrm{tot}} = (1 \mp j) l E_x^{\mathrm{loc}}. \tag{81}$$

Respectively, the induced current at the point where the dipole connects to the loop is

$$I_{\mathrm{dip}} = \frac{(1 \mp j) l E_x^{\mathrm{loc}}}{Z_{\mathrm{dip}} + Z_{\mathrm{loop}}}, \tag{82}$$

where Z_{dip} is the input impedance of the dipole and Z_{loop} is the input impedance of the loop. The induced electric and magnetic dipole moments are proportional to this current:

$$p_{\mathrm{e},x} = \frac{I_{\mathrm{dip}} l}{j\omega} = -j\frac{(1 \mp j) l^2 E_x^{\mathrm{loc}}}{\omega(Z_{\mathrm{dip}} + Z_{\mathrm{loop}})}, \tag{83}$$

$$p_{\mathrm{m},y} = \mu_0 I_{\mathrm{dip}} S = \eta_0 \frac{(1 \mp j) l^2 E_x^{\mathrm{loc}}}{\omega(Z_{\mathrm{dip}} + Z_{\mathrm{loop}})}, \tag{84}$$

where we use the fact that $S = l/k_0$ if $h_{\mathrm{loop}} = h_{\mathrm{dip}} = l$. When the particle is at resonance, $Z_{\mathrm{dip}} + Z_{\mathrm{loop}} = 2R_{\mathrm{rad}} + R_{\mathrm{loss}}$, where $R_{\mathrm{rad}} = \frac{\eta_0 k_0^2 l^2}{6\pi}$ is the radiation resistance of a short dipole antenna (when $h_{\mathrm{loop}} = h_{\mathrm{dip}}$ both antennas have the same radiation resistance) and R_{loss} corresponds to the ohmic loss in metal, which we may neglect. From these relations we see that the induced dipole moments in the linear omega particle are in quadrature.

However, from (70)–(71) it follows, first, that in the nonlinear particle which we want to design the contributions due to $\mathbf{E}^{\mathrm{loc}}$ and $\mathbf{H}^{\mathrm{loc}}$ in the expressions for both dipole moments must be in phase (for the wave incident from $z < 0$), and, second, the induced electric and magnetic moments themselves must be also in phase. In a symbolic language, we may say that the four-pole network that we insert between the two antennas must act in such a way that $\mp j$ in (83)–(84) is replaced with ± 1, and η_0 in (84) with $-j\eta_0$. As will be seen in a few moments, this can be achieved with microwave nonlinear circuits known as *balanced modulators* (BM).
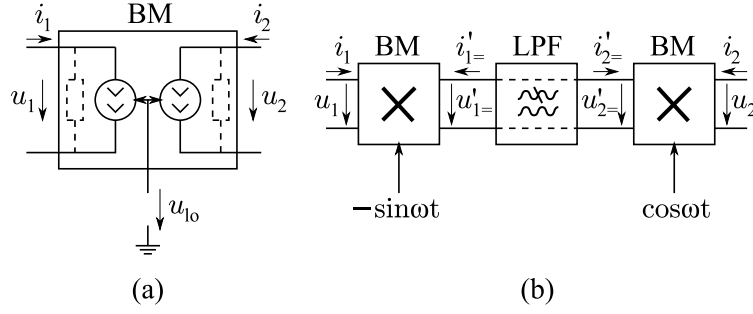
FIG. 2: (a) Equivalent circuit of an idealized balanced modulator (BM). (b) A network composed of two balanced modulators connected through a low-pass filter (LPF).

A balanced modulator is a three-port device such that there are two ports that may both serve as input and output (the ports are exchangeable due to the symmetry of the circuit; that is one of the reasons why the circuit is called *balanced* modulator), and the third port to which a voltage from a local oscillator is applied. The function that the BM performs is a multiplication of the signal applied to one of its input ports and the signal of the local oscillator. One may represent an idealized BM with an equivalent circuit shown in Fig. 2(a). The controllable current sources in the circuit depend on the instantaneous voltages at the ports as follows:

$$i_1(t) = K_{12} u_2(t) u_{\text{lo}}(t), \tag{85}$$

$$i_2(t) = K_{21} u_1(t) u_{\text{lo}}(t), \tag{86}$$

where $u_{\text{lo}}(t)$ is the voltage at the local oscillator port and $u_{1,2}(t)$ and $i_{1,2}(t)$ are the voltages at the other two ports. We need power conserving BMs which do not absorb or store power that is delivered to ports 1 and 2, hence, $u_1(t)i_1(t) + u_2(t)i_2(t) = 0$. From here, $K_{12} = -K_{21}$. The input and output resistances of the BM shown in the figure with dashed lines are assumed to be very large and are not taken into account.

Consider now the network depicted in Fig. 2(b). In this network we have connected two BMs through a low-pass filter (LPF). One may imagine this LPF as a Π-type CLC-filter with an inductor in a series branch and two capacitors in the parallel branches. For us, however, the only thing that is important here is that this LPF freely passes through the direct-current (DC) component and blocks all high-frequency components (the DC path through the filter is shown with dashed lines).

The whole network is designed to operate with signals at the frequency $\omega = 2\pi f_0 = 2\pi/T_0$, therefore, we may represent the voltages $u_{1,2}(t)$ as

$$u_{1,2}(t) = U_{1,2}^{\text{re}} \cos \omega t - U_{1,2}^{\text{im}} \sin \omega t. \tag{87}$$

We apply the local oscillator signal at the frequency ω and the phase $\varphi = \pi/2$ to the first BM: $u_{\text{lo},1} = -\sin \omega t$, and another signal at the same frequency and $\varphi = 0$ to the second BM: $u_{\text{lo},2} = \cos \omega t$. Therefore, we may write for the DC currents $i'_{1,2=}$ (here $\langle \ldots \rangle_{T_0}$ denotes averaging over a period):

$$i'_{1=} = K_{21} \left\langle (U_1^{\text{re}} \cos \omega t - U_1^{\text{im}} \sin \omega t)(-\sin \omega t) \right\rangle_{T_0} = \frac{1}{2} K_{21} U_1^{\text{im}}, \tag{88}$$

$$i'_{2=} = K_{12} \left\langle (U_2^{\text{re}} \cos \omega t - U_2^{\text{im}} \sin \omega t) \cos \omega t \right\rangle_{T_0} = \frac{1}{2} K_{12} U_2^{\text{re}}. \tag{89}$$

But as is dictated by the topology of the network, $i'_{1=} = -i'_{2=}$, therefore,

$$U_1^{\text{im}} = U_2^{\text{re}}. \tag{90}$$

Next, we express the high-frequency currents at the ports 1 and 2:

$$i_1(t) = (K_{12} u'_{1=})(-\sin \omega t) = -I_1^{\text{im}} \sin \omega t, \tag{91}$$

$$i_2(t) = (K_{21} u'_{2=}) \cos \omega t = I_2^{\text{re}} \cos \omega t, \tag{92}$$

where $I_1^{\text{im}} = K_{12} u'_{1=}$ and $I_2^{\text{re}} = K_{21} u'_{1=}$. But again, from the topology of the network, the DC voltages satisfy $u'_{1=} = u'_{2=}$, therefore,

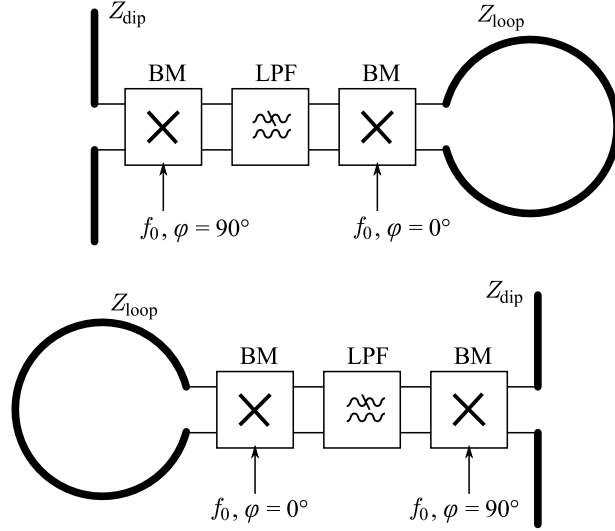$$I_1^{\text{im}} = -I_2^{\text{re}}. \tag{93}$$

FIG. 3: The topology of the two types of phase conjugating bi-anisotropic inclusions for the phase conjugating surface operating at the frequency f_0. Each particle consists of a short dipole antenna with the impedance Z_{dip} and a small loop antenna with the impedance Z_{loop}. The two antennas are interconnected through a nonlinear and nonreciprocal network composed of two balanced modulators (BM) and a low-pass filter (LPF). The mixers are fed by a local oscillator with two signal outputs in quadrature $\varphi = 0°$ and $\varphi = 90°$. See the main text for further explanations.

Notice also that always $I_1^{\text{re}} = I_2^{\text{im}} = 0$.

Thus, from (90) and (93) it is evident that the considered network operates, essentially, as a "connector" between the imaginary current and voltage at the first port, and the real current and voltage at the second port. The network also enforces zero real current in the first port and zero imaginary current in the second port. This is exactly what we need in the design of the phase conjugating particles, and the corresponding topologies including the antennas are shown in Fig. 3.

In these designs we connect the dipole and loop antennas to the BM-based network discussed above. The electrical size of the circuit is negligible, and both antennas are excited by the same local field. Let us analyze the operation of the variant shown at the top of Fig. 3. First of all, it is evident that when placed in an arbitrary local field, the EMFs in both antennas are still given by (78) and (79). However, contrary to what happens in a linear omega particle, the real part of $\mathcal{E}_{\text{dip}}$ and the imaginary part of $\mathcal{E}_{\text{loop}}$ will not be able to excite any current in the antennas, because these components are blocked by the BMs. Therefore, the relevant parts of the EMFs in the two antennas are (as above, we let $h_{\text{dip}} = h_{\text{loop}} = l$)

$$\mathcal{E}_{\text{dip}}^{\text{im}} = l\,\text{Im}(E_x^{\text{loc}}), \tag{94}$$

$$\mathcal{E}_{\text{loop}}^{\text{re}} = \eta_0 l\,\text{Im}(H_y^{\text{loc}}). \tag{95}$$

Analogously, the voltage drops on the reactive parts $X_{\text{dip}} = \text{Im}(Z_{\text{dip}})$ and $X_{\text{loop}} = \text{Im}(Z_{\text{loop}})$ of the input impedances of the dipole and the loop have no effect as well, as they are in quadrature with respect to the current flowing through them. Thus, the only relevant part of the input impedance is the radiation resistance.

From the topology of the network, $I_{\text{dip}}^{\text{im}} = -I_1^{\text{im}}$ and $I_{\text{loop}}^{\text{re}} = I_2^{\text{re}}$, therefore, $I_{\text{dip}}^{\text{im}} = I_{\text{loop}}^{\text{re}}$. Next, because of (90), the EMFs (94) and (95) and the rest of the equivalent circuits of the two antennas (only two R_{rad} remain) appear to be essentially connected in series, hence,

$$I_{\text{dip}}^{\text{im}} = I_{\text{loop}}^{\text{re}} = \frac{l[\text{Im}(E_x^{\text{loc}}) + \eta_0\,\text{Im}(H_y^{\text{loc}})]}{2R_{\text{rad}}}. \tag{96}$$

The complex amplitudes of the electric and magnetic dipole moments, therefore, read

$$p_{\text{e},x} = \frac{l(jI_{\text{dip}}^{\text{im}})}{j\omega} = \frac{l^2}{2\omega R_{\text{rad}}}[\text{Im}(E_x^{\text{loc}}) + \eta_0\,\text{Im}(H_y^{\text{loc}})], \tag{97}$$

$$p_{\text{m},y} = \mu_0 I_{\text{loop}}^{\text{re}} S = \eta_0 \frac{l^2}{2\omega R_{\text{rad}}}[\text{Im}(E_x^{\text{loc}}) + \eta_0\,\text{Im}(H_y^{\text{loc}})], \tag{98}$$
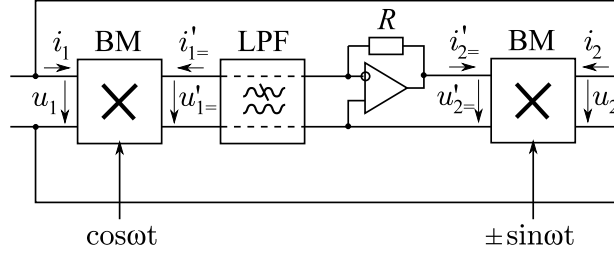
FIG. 4: A nonlinear single-port network used as a load for a short electric dipole. The network is composed of the same elements as in Fig. 2, with an additional operational amplifier working in the current-to-voltage conversion mode.

which is a particular case of (70)–(71) for the considered polarization.

As can be readily verified, the second design variant shown at the bottom of Fig. 3 has the opposite signs of the magnetoelectric interaction terms, and, thus, must be used to conjugate the plane waves incident from the half space $z > 0$.

B. Case of evanescent waves

To phase-conjugate the evanescent waves, the particles must react to the real parts of electric and magnetic fields, as follows from (64)–(65). In this case the inclusions are simple electric and magnetic dipoles without magneto-electric interaction. Therefore, as the base for our design we may choose the loaded dipole and loop antennas. In what follows, we consider in detail the case of a linear electric dipole oriented along the x-axis (the magnetic dipole along the y-axis may be considered in a dual manner).

When a short loaded dipole is placed in an electric field, an EMF is induced in the dipole, with the value given by (78). Respectively, the current induced in the dipole is

$$I_{\mathrm{dip}} = \frac{l E_x^{\mathrm{loc}}}{Z_{\mathrm{dip}} + Z_{\mathrm{load}}}, \tag{99}$$

where Z_{load} is the impedance of a bulk load connected to the dipole. The induced electric dipole moment of the loaded dipole reads

$$p_{\mathrm{e},x} = \frac{I_{\mathrm{dip}} l}{j\omega} = -j \frac{l^2 E_x^{\mathrm{loc}}}{\omega(Z_{\mathrm{dip}} + Z_{\mathrm{load}})}. \tag{100}$$

It is easy to verify that if we chose the load so that

$$Z_{\mathrm{load}} = -Z_{\mathrm{dip}} + \frac{j\eta_0 l^2}{A_0} \mathrm{Im}(\beta), \tag{101}$$

then the condition for the surface electric current polarizability (64) in an array of such particles will be satisfied, with an exception that the linear particles will react to both real and imaginary parts of the electric field.

With the use of BMs we may get rid of the reaction to the imaginary part of the field and also find a simple way to realize the necessary loading (101). Consider the network shown in Fig. 4. This network is similar to the ones we considered in Sec. IV A. It is composed of a pair of BMs and a LPF, with an additional element in the middle that is an operational amplifier working in the current-to-voltage conversion mode. We pump the first BM at the frequency f_0 with the phase $\varphi = 0$, and the second one with the phase $\varphi = \pm\pi/2$ (it will be seen soon why we consider two signs of the phase). The output of the network is directly connected to its input, so that the circuit is essentially a single port device that may be used as an active load. To analyze the operation of the circuit we first notice that because the voltage at the input of the operational amplifier is negligibly small, $u'_{1=} = 0$, and, therefore, $i_1 = 0$. Next, assuming that the voltage at the input of the circuit is $u_1 = U_1^{\mathrm{re}} \cos\omega t - U_1^{\mathrm{im}} \sin\omega t$, $\omega = 2\pi f_0 = 2\pi/T_0$, we obtain

$$i'_{1=} = K_{21} \left\langle (U_1^{\mathrm{re}} \cos\omega t - U_1^{\mathrm{im}} \sin\omega t) \cos\omega t \right\rangle_{T_0} = \frac{1}{2} K_{21} U_1^{\mathrm{re}}. \tag{102}$$

Hence, the DC voltage at the output of the operational amplifier is

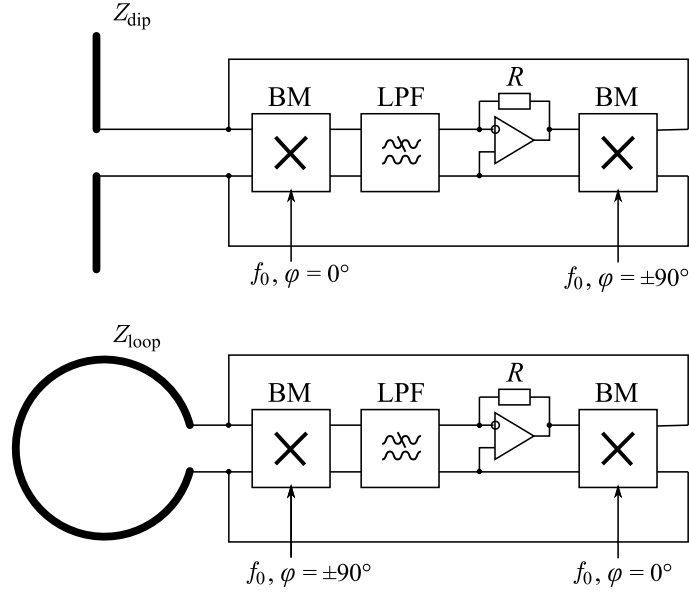$$u'_{2=} = i'_{1=} R = \frac{1}{2} K_{21} R U_1^{\mathrm{re}}, \tag{103}$$

FIG. 5: The topology of the two particles loaded with nonlinear circuits designed to operate with the evanescent part of the spatial spectrum. Top: a short electric dipole loaded with a nonlinear load. Bottom: a small magnetic loop loaded with a nonlinear load.

where R is the resistor in the feedback loop of the operational amplifier. Therefore,

$$i_2(t) = \mp K_{21} u'_{2=} \sin \omega t = \mp \frac{1}{2} K_{21}^2 R U_1^{\mathrm{re}} \sin \omega t = -I_2^{\mathrm{im}} \sin \omega t, \qquad (104)$$

where $I_2^{\mathrm{im}} = \pm K_{21}^2 R U_1^{\mathrm{re}}/2$. This current is the input current of the whole network, because the input current of the first BM equals zero. Thus, we have designed a circuit in which a real input voltage induces an imaginary current, i.e., the circuit behaves almost as a usual reactance (the plus sign in the expression for the current corresponds to the capacitance and the minus sign — to the inductance), with the difference that the loading circuit is not sensitive at all to the imaginary input voltage. This is exactly what we need to realize the nonlinear particles reacting only to the real part of the electric field. Indeed, to realize the required loading one has to choose the parameters of the circuit so that

$$\pm \frac{1}{2} K_{21}^2 R = -X_{\mathrm{dip}} + \frac{\eta_0 l^2}{A_0} \mathrm{Im}(\beta). \qquad (105)$$

It is interesting to note that there is no need to compensate the real part of the dipole impedance Z_{dip} (the radiation resistance), because the circuit reacts only to the real part of the input voltage, and the additional voltage drop on the radiation resistance $U_R = jI_2^{\mathrm{im}} R_{\mathrm{rad}}$ is purely imaginary.

An example topology of an electric dipole particle with the nonlinear active load is shown in Fig. 5, top, and the same for the magnetic dipole particle in Fig. 5, bottom (notice the difference in phases of the local oscillator signals in both schematics). We would like to stress that the operational amplifier seen in this schematic works with a DC signal. Thus, its role is *not* to amplify the evanescent fields of an incoming wave, but just to provide the necessary *reactance* of the loading circuit in order to tune the structure to a resonance. In turn, the evanescent modes in this structure are enhanced because of this resonance.

V. CONCLUSIONS

In this paper, the concept of perfect lensing with a pair of phase conjugating surfaces introduced by us earlier,[8] i.e., a possibility to achieve optical resolution well below the wavelength limit without using double-negative materials, has been further developed. Working as a planar lens, a pair of phase conjugating sheets is able to focus propagating modes of a source due to the negative refraction at the interfaces and, in the same time, enhance the evanescent modes due to surface plasmon-polariton resonances, i.e., it provides sub-wavelength resolution imaging indistinguishable from the perfect lens proposed by Pendry, while not suffering from its known drawbacks.

We have investigated in detail the physics of operation of nonlinear sheets with the boundary conditions of the form $\mathbf{E}_t(\omega)|_1 = \mathbf{E}_t(\omega)^*|_2$, $\mathbf{H}_t(\omega)|_1 = \mathbf{H}_t(\omega)^*|_2$ and have demonstrated that they are, in principle, physically realizable with devices imposing the necessary relations between the fields and the equivalent electric and magnetic surface currents at the phase conjugating boundary. Namely, we have shown that the mentioned surface currents must form Huygens sources that radiate towards a given side of the boundary, negating the fields incident from the other side and creating complex-conjugated fields in the corresponding half space.

As a possible realization of such sheets, we have proposed and considered in this paper arrays of nonlinear and nonreciprocal bi-anisotropic inclusions reacting differently to the propagating and evanescent plane waves. At microwaves, the considered design makes use of balanced modulators (a type of mixers) to provide for the required nonlinearity and nonreciprocity of the circuit. At optics, a design utilizing similar principles may become feasible in future as the field of optical nanocircuits develops further.

As a final note we would like to mention that in such arrays the enhancement of the evanescent waves is due to a high-quality surface mode resonance, as in the grids of passive resonant inclusions considered in Ref. 3. This is in contrast to Ref. 10 where the phase conjugating surface must itself parametrically amplify the fields which requires an unphysically high conversion efficiency.

[1] J. Pendry, Negative refraction makes a perfect lens, *Phys. Rev. Lett.,* vol. 85, pp. 3966–3969, 2000.

[2] V. Veselago, The electrodynamics of substances with simultaneously negative values of ϵ and μ, *Sov. Phys. Usp.,* vol. 10, pp. 509–514, 1968.

[3] S. Maslovski, S. Tretyakov, and P. Alitalo, Near-field enhancement and imaging in double planar polariton-resonant structures, *J. Appl. Phys.,* vol. 96, no. 3, pp. 1293–1300, 2004.

[4] M. J. Freire and R. Marqués, Planar magnetoinductive lens for three-dimensional subwavelength imaging, *Appl. Phys. Lett.,* vol. 86, pp. 182505(1–3), 2005.

[5] P. Alitalo, S. Maslovski, and S. Tretyakov, Near-field enhancement and imaging in double cylindrical polariton-resonant structures: Enlarging superlens, *Phys. Lett. A,* vol. 357, pp. 397–400, 2006.

[6] P. Alitalo, C. Simovski, A. Viitanen, and S. Tretyakov, Near-field enhancement and subwavelength imaging in the optical region using a pair of two-dimensional arrays of metal nanospheres, *Phys. Rev. B,* vol. 74, p. 235425(1–6), 2006.

[7] S. Maslovski, P. Alitalo, and S. Tretyakov, Subwavelength imaging based on frequency scanning, *J. Appl. Phys.,* vol. 104, p. 103109(1–5), 2008.

[8] S. Maslovski and S. Tretyakov, Phase conjugation and perfect lensing, *J. Appl. Phys.,* vol. 94, no. 7, pp. 4241–4243, 2003.

[9] C. A. Allen, K. M. K. H. Leong, and T. Itoh, A negative reflective/refractive "meta-interface" using a bi-directional phase-conjugating array, *IEEE Int. Microw. Theory Techn. Symp. Digest,* vol. 3, pp. 1875–1878, 2003.

[10] J. B. Pendry, Time reversal and negative refraction, *Science,* vol. 322, pp. 71–73, 2008.

[11] V. F. Fusco, N. B. Buchanan, and O. Malyuskin, Active phase conjugating lens with sub-wavelength resolution capability, *IEEE Trans. Antennas Propagat.,* vol. 58, pp. 798–808, 2010.

[12] A. R. Katko, S. Gu, J. P. Barrett, B. Popa, G. Shvets, and S. A. Cummer, Phase conjugation and negative refraction using nonlinear active metamaterials, *Phys. Rev. Lett.,* vol. 105, p. 123905, 2010.

[13] A. Alù and N. Engheta, Physical insight into the "growing" evanescent fields of double-negative metamaterial lenses using their circuit equivalence, *IEEE Trans. Antennas Propagat.,* vol. 54, no. 1, pp. 268–272, 2006.

[14] I. Lindell, *Methods for electromagnetic field analysis,* Piscataway, NJ: IEEE Press, 1995.

[15] S. I. Maslovski and S. A. Tretyakov, Full-wave interaction field in two-dimensional arrays of dipole scatterers, *Int. J. Electronics and Communications (AEÜ),* vol. 53, no. 3, pp. 135–139, 1999.

[16] S. A. Tretyakov, A. J. Viitanen, S. I. Maslovski, and I. E. Saarela, Impedance boundary conditions for regular dense arrays of dipole scatterers, *IEEE Trans. Antennas Propagat.,* vol. 51, no. 8, pp. 2073–2078, 2003.

[17] S. A. Tretyakov, A. H. Sihvola, A. A. Sochava, and C. R. Simovski, Magnetoelectric interactions in bi-anisotropic media, *J. Electromagnetic Waves App.,* vol. 12, no. 4, pp. 481–497, 1998.

[18] A. N. Serdyukov, I. V. Semchenko, S. A. Tretyakov, and A. Sihvola, *Electromagnetics of bi-anisotropic materials: Theory and applications,* Amsterdam: Gordon and Breach Science Publishers, 2001.

[19] M. M. I. Saadoun and N. Engheta, A reciprocal phase shifter using novel pseudochiral or Ω medium, *Microw. and Opt. Technol. Lett.,* vol. 5, pp. 184–188, 1992.

[20] S. A. Tretyakov, A. A. Sochava, Proposed composite material for non-reflecting shields and antenna radomes, *Electronics Letters,* vol. 29, no. 12, pp. 1048–1049, 1993.